

# A New Approach in Optimizing the Induction Heating Process Using Flux Concentrators: Application to 4340 Steel Spur Gear

*Noureddine Barka, Ahmed Chebak, Abderrazak El Ouafi, Mohammad Jahazi, and Abdellah Menou*

*(Submitted February 20, 2014; in revised form May 6, 2014; published online June 7, 2014)*

The beneficial effects of using flux concentrators during induction heat treatment process of spur gears made of 4340 high strength steel is demonstrated using 3D finite element model. The model is developed by coupling electromagnetic field and heat transfer equations and simulated by using Comsol software. Based on an adequate formulation and taking into account material properties and process parameters, the model allows calculating temperature distribution in the gear tooth. A new approach is proposed to reduce the electromagnetic edge effect in the gear teeth which allows achieving optimum hardness profile after induction heat treatment. In the proposed method, the principal gear is positioned in sandwich between two other gears having the same geometry that act as flux concentrators. The gap between the gear and the flux concentrators was optimized by studying temperature variation between the tip and root regions of gear teeth. Using the proposed model, it was possible identifying processing conditions that allow for quasi-uniform final temperature profile in the medium and high frequency conditions during induction hardening of spur gears.

**Keywords** 3D model, high frequency and medium frequency, induction heating, spur gear

## 1. Introduction

The main failure modes of gears in service are the flank wear, bending fatigue, contact fatigue (pitting). Careful analysis of these failure modes can help to understand the various phenomena involved and to propose appropriate technological improvements to enhance mechanical behavior of these components (Ref 1, 2). Wear is defined as local phenomenon, characterized by the removal of material caused by the relative movement of sliding contact surfaces. While the slip is low in the region near the pitch circle, the wear is greatest near the tip and the root. To overcome this phenomenon, it is important to ensure the best possible lubrication conditions and to increase the surface hardness of the teeth.

Bending fatigue is essentially caused by the alternating stresses generated at the root. During its passage through the meshing, the active edge of each tooth undergoes a loading cycle which generates an alternative tensile and compression stress. The loaded side of the tooth is being in tension thereby promoting crack initiation and propagation. To improve bending fatigue life, it is necessary to

generate compressive residual stresses at the tooth root to a sufficient depth. These stresses have a beneficial effect on the gear endurance since they limit the initiation and propagation of cracks in areas under tension (Ref 2). Contact fatigue damage is created in active flank areas under the action of repeated contact that generates cyclic stresses. The contact surfaces are subjected to complex stress field while slipping and rolling in the meshing. Compressive stress is maximal at the center and the surface of the contact region. In addition, the maximum shear stress is below the surface, to a depth equal to approximately one-third of the average width of the contact region. Thus, each contact surface records a cycle of compression and tension which can lead to surface damage. It is recognized that shear stresses which attain their maximum in the subsurface region, may cause cracks that propagate to the surface and cause pitting (Ref 2). To improve contact fatigue resistance, it is necessary to produce a surface layer having a hard and fine-grained microstructure on a sufficiently large depth. Indeed, the surface hardness appears to be beneficial to delay the crack initiation since there is a relationship between the hardness of a material and its endurance limit (Ref 3). The presence of a thin martensitic layer is beneficial for fatigue performance as it significantly delays crack propagation (Ref 4). In fact, during induction heating, residual stresses are generated by the temperature gradient which induces inducing uneven and thermal expansions in the material. They are also created by the difference in volume between the martensite and austenite. The generation of compressive residual stresses during induction heating will have a beneficial effect on the fatigue behavior of mechanical components (Ref 5).

In the automotive and aerospace industries, it is necessary to define some design specifications based on strength calculations to obtain the optimum performance of mechanical components. Specifically, the hardness profile of the spur gear must ideally be uniform at the tip and the root of the teeth. However, it is difficult to reach this goal based only on the combination of machine

**Noureddine Barka, Ahmed Chebak, and Abderrazak El Ouafi**, Mathematics, Computer Science and Engineering Department, University of Quebec at Rimouski, Rimouski, QC, Canada; **Mohammad Jahazi**, Mechanical Engineering Department, École de technologie supérieure, Montreal, QC, Canada; and **Abdellah Menou**, International Academy of Civil Aviation, Casablanca, Morocco. Contact e-mail: noureddine\_barka@uqar.ca.

parameters and/or on the change of coil geometry. A 3D model coupling the electromagnetic field and the thermal transfer is a promising solution for reliable investigating the induction heating process. Such models would allow better understanding and confirmation of the experiments applied to this type of gear with higher precision than a 2D model. Literature review has demonstrated that simulation models have been developed and allow for the analysis of the hardness profile as a function of material properties or in terms of machine parameters. Several studies conducted by some authors have concluded that for a reliable and accurate prediction of the hardening process, it is important to find another method to control the heating at the edge (edge effect) (Ref 6, 7). Specifically, in a previous work, the authors have reported on the beneficial effects of flux concentrators for disk shape geometries using an axisymmetric model (Ref 8). It will be interesting to apply the technique to validate its applicability in the case of gear in a 3D model. This approach consists in taking the principal gear to be heat treated in sandwich by two other thin gears having the same geometry and acting as flux concentrators. From an industrial perspective, the application of flux concentrators will bring higher quality, more flexibility, and cost reduction as these concentrators could be reused several times before they have to be replaced.

The aim of this work is to investigate the effect of adding flux concentrators to spur gear using 3D simulation for medium frequency (MF) and high frequency (HF) cases. The first step is to develop the model, discuss on temperature profile, and validate it by using experimental data as in Ref 6. In the second step, the effect of the gap between the gear and the flux concentrators ( $Gap_z$ ) on the temperature at the surface is studied and the optimal gap is found. Finally, the MF and HF powers are mixed by sequential mode to reach the optimum temperature profile able to approximate the hardness profile.

## 2. Initial Model (Without Flux Concentrators)

The global system of electromagnetic equations is based on the Maxwell's equations that are combined with constitutive

relations that introduce the electromagnetic properties. Considering the magnetic potential vector formulation ( $A$ ) and neglecting the hysteresis and magnetic saturation, the general equation governing the electromagnetic behavior can be expressed as Ref 9, 10

$$\frac{1}{\mu(T)} \nabla^2 A = -j\omega\sigma(T)A + J_0. \quad (\text{Eq 1})$$

The electromagnetic problem resolution is used to calculate the energy generated during induction heating. The heat ( $Q_{\text{Ind}}$ ), generated in the surface layer, can be expressed as function of the magnetic potential vector (Ref 9, 10)

$$Q_{\text{Ind}} = \frac{(\nabla^2 A)^2}{\mu(T)\sigma(T)}. \quad (\text{Eq 2})$$

The heat transfer mechanism can be described by Fourier-Kirchhoff equation. The thermal analysis is coupled with the electromagnetic problem using equation (Ref 3, 11, 12)

$$k(T)\nabla^2 T = \gamma C_p(T) \frac{\partial T}{\partial z} + \dot{Q}_{\text{Ind}}. \quad (\text{Eq 3})$$

The current model considers a spur gear with  $\text{Ø } 102.5$  mm external diameter,  $\text{Ø } 80$  mm internal diameter, 6.5 mm thickness and having 48 teeth with a module 2. The coil is represented by a square ring section made of copper ( $7 \text{ mm} \times 7 \text{ mm} = 49 \text{ mm}^2$ ) and the gap between the gear and the coil is fixed to 2.00 mm. Moreover, only gear and coil quarters are considered in the simulation in order to refine the mesh quality, increase the precision, and reduce computation time (Fig. 1). The material (4340 steel) is regarded as homogeneous and isotropic. The electromagnetic and thermal properties are pondered in this model in function of the heating temperature. In fact, relative magnetic permeability, electrical conductivity, thermal conductivity, and specific heat are considered in this study (Ref 13). The main components are surrounded by a local dielectric environment that is magnetically isolated along with vacuum permittivity and permeability. Electrical insulation and thermal insulation are regarded at middle plan. Magnetic insulation and thermal insulation are respected at boundaries

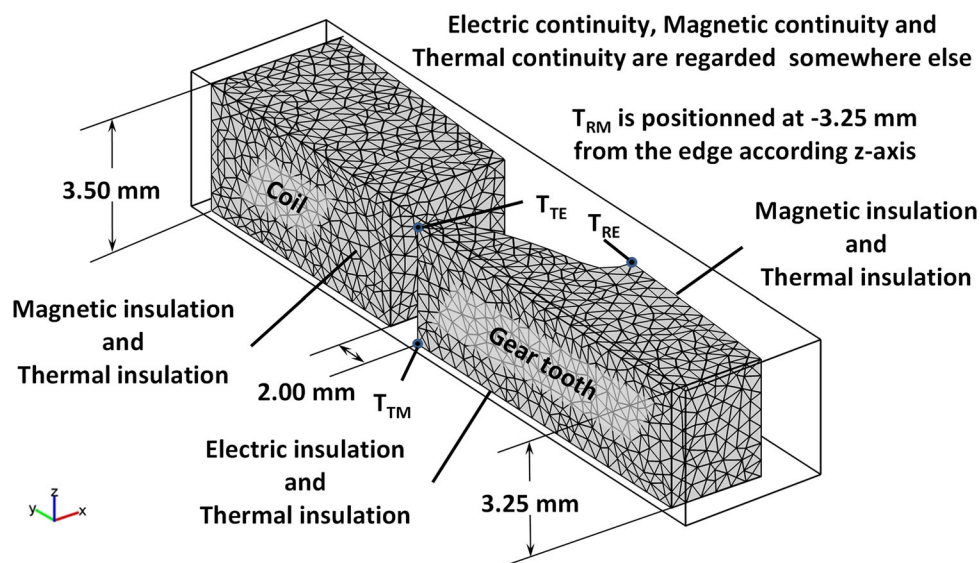


Fig. 1 Model without flux concentrator—final mesh

created by cutting plan limiting the half tooth geometry. Electrical continuity, magnetic continuity, and thermal continuity are observed somewhere else. Heat losses by convection and radiation modes are assumed equivalent to conduction in the air at the interface due to the very short time of treatment. The mesh is dense inside the part and the coil due to the high induced currents and temperature gradients between the surface and the core. A convergence study was conducted and it provides a model with optimized mesh having 0.25 mm size in the gear and in the coil. The four temperatures considered in the gear tooth are  $T_{RE}$  and  $T_{RM}$  at the root (edge and middle plan) and  $T_{TE}$  and  $T_{TM}$  at the tip (edge and middle plan), as shown in Fig. 1.

Tables 1 and 2 present the simulation and experimental machine parameters for the preliminary tests. The simulation and the experimental tests are done and compared together. The frequencies and heating time remains, but the machine power is compared to the power consumed by the part calculated by simulation. Once the validation is performed and the model is developed, the imposed current density ( $J_0$ ) is tuned to have the same hardness profile based on the temperature distribution.  $J_0$  is adjusted at  $2.10 \times 10^{10}$  A/m<sup>2</sup> in MF case (10 kHz) and  $6.25 \times 10^{10}$  A/m<sup>2</sup> in HF case (200 kHz). The heating time is fixed at 0.50 s.

A brief review of results, presented in Fig. 2, confirm that when MF is applied, the majority of the heat is generated around the root region where the temperature reaches maximal value, while the temperature in the tip region remains low. However, when HF is used, the induced currents generate much more heat in the tip and pitch diameter regions (Fig. 3). One can notice also that the edge effect is very obvious and the root is highly heated at the gear edge. Overall, the simulation results show that only the root region and a small region around can be transformed into hard martensite when the MF is applied in the edge and at the middle plan. The obtained results confirms that the temperature using MF power attain 1170 °C at the end heating and only 1050 °C in the HF case. By contrast, if HF is employed, the high temperature distribution covers the contour on the tooth including the root at the edge; while at the middle plan, only the tip region and a small area close to the pitch diameter are heated above  $A_{c3}$  (Fig. 3). In fact, due to its good hardenability of 4340 steel, it is possible to transform all region heated above  $A_{c3}$  to hard martensite even if the cooling is at air free convection. As the critical cooling rate to form martensite from austenite for the steel used in this research, work (4340 steel) was about 30 °C/s, the conciliator assumption was quite realistic in this case (Ref 14). Using this approximation, the experimental tests show that there is a good concordance

**Table 1** Validation tests parameters

Test	Frequency (kHz)	Heating time (s)	Power (kW)
1	10	0.50	220
2	200	0.50	83

**Table 2** Simulation parameters

Test	Frequency (kHz)	Heating time (s)	$J_0$ (A/m <sup>2</sup> )
1	10	0.50	$2.10 \times 10^{10}$
2	200	0.50	$6.25 \times 10^{10}$

between the simulation results (temperature profile) and the experiments (hardness profile) in both MF and HF cases. In fact, The MF power transforms the root and the region surrounding into hard martensite and almost equal at the edge and middle plan (Fig. 4). However, the HF power generates a contour hardness profile at the edge and transforms only the tooth body without affecting the root at the middle plan (Fig. 5).

Figures 6 and 7 present the four temperatures at the end of heating (0.5 s) in the MF and HF cases, respectively. In both cases, an offset is recorded between temperatures in the root ( $T_{RM}$  and  $T_{RE}$ ). However,  $T_{TM}$  and  $T_{TE}$  remain very close. At the end of heating, the offset between the temperatures  $T_{RE}$  and  $T_{RM}$  is about 150 °C and the difference between  $T_{TE}$  and  $T_{TM}$  is less than 40 °C in MF case. In HF case, the difference between root temperatures is more important (230 °C) and the temperatures are almost the same at the tip. The above results indicate that, the edge effect is present in the root and must be considered, while it is negligible in the gear tip. The simulation

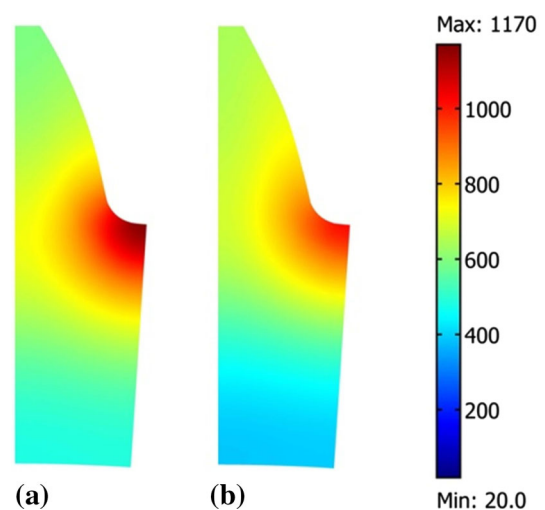


**Fig. 2** Final temperature distribution (°C): (a) Edge and (b) Middle plan—MF

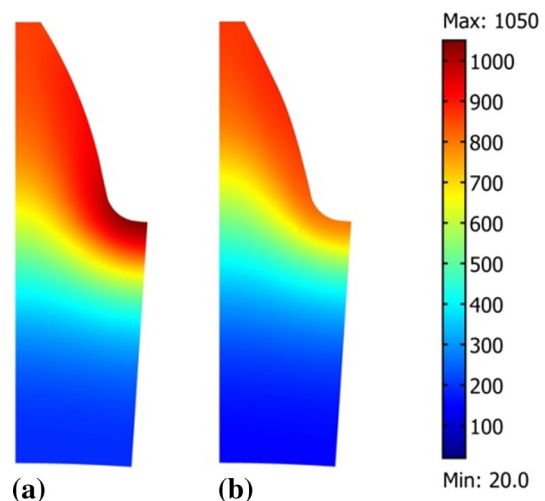


**Fig. 3** Final temperature distribution (°C): (a) Edge and (b) Middle plan—HF

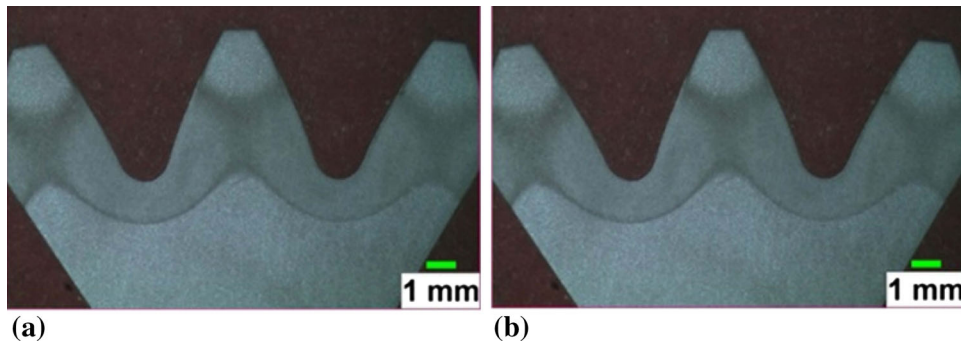


Fig. 4 Experimental hardness profile: (a) Edge and (b) Middle plan—MF

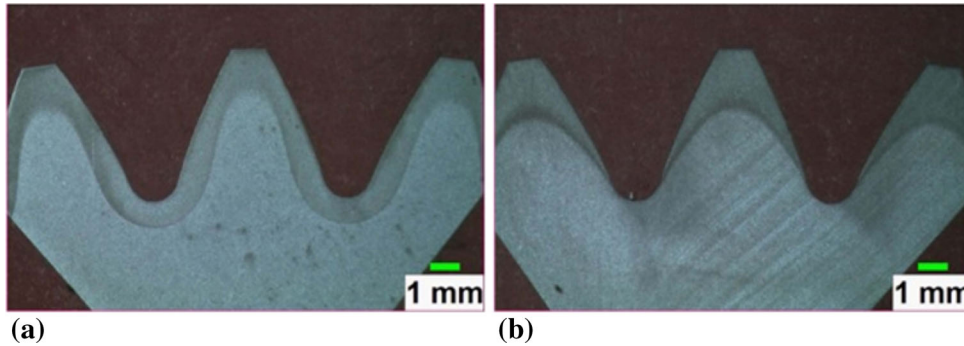


Fig. 5 Experimental hardness profile: (a) Edge and (b) Middle plan—HF

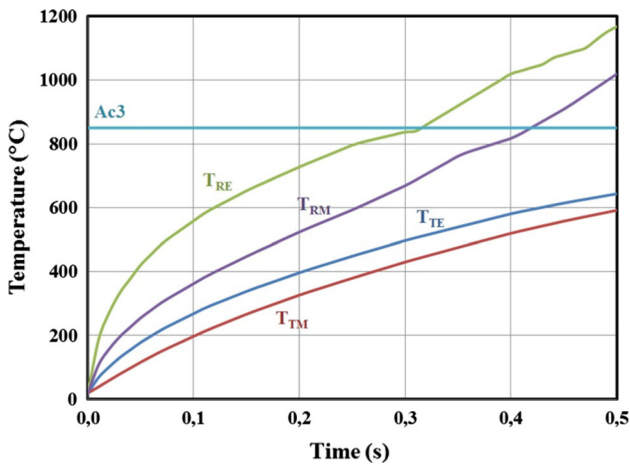


Fig. 6 Temperatures vs. time—MF

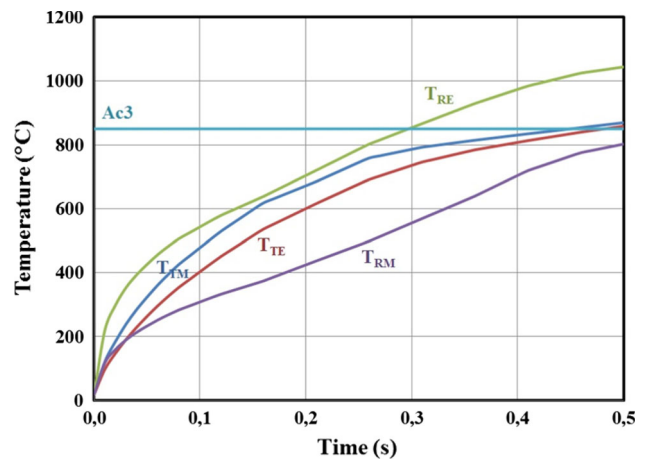


Fig. 7 Temperatures vs. time—HF

results confirm also that the root (Edge) is completely austenitized before the other during MF and HF heating.

### 3. Reduction of Edge Effect (Model with Flux Concentrators)

The second model uses the same gear and coil presented previously. In this case, two flux concentrators having the same geometry than the initial gear but with half thickness of this one were added to the assembly. The boundary conditions, mesh

characteristics, and operational conditions are similar to the previous case (Fig. 8). In this case, the model includes gear, flux concentrators, coil, and environment. The following model is composed of reduced component like the first model. In fact, using symmetric condition (electric insulation and thermal insulation) allows using the half of the gear and coil and one flux concentrator. The periodic condition (magnetic insulation and thermal insulation) allows reducing the half to a quarter. This size reduction is important to execute computation in less time and then increase the mesh quality. Note that the continuity conditions are regarded somewhere else. The distance  $Gap_z$  is varied then in order to study the effect of this parameter on the

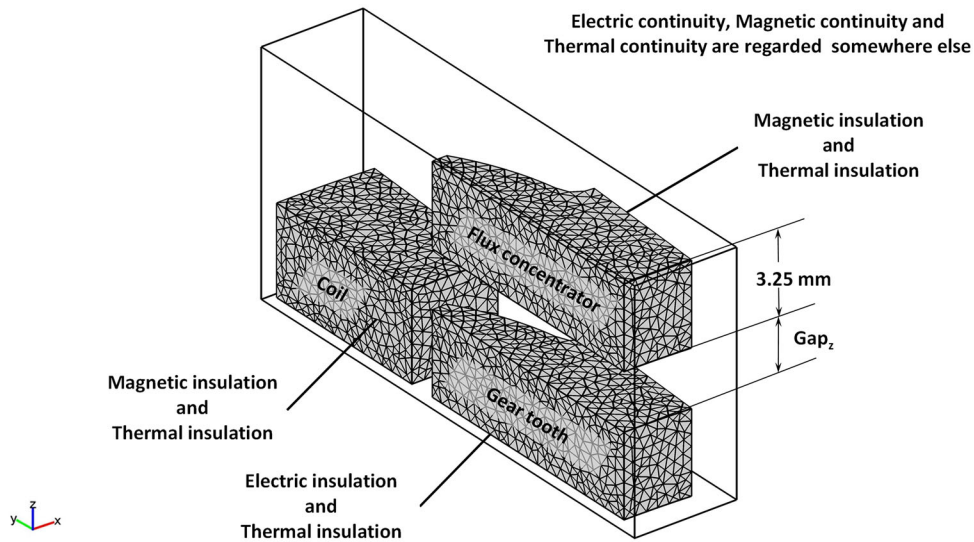


Fig. 8 Model with flux concentrator—final mesh

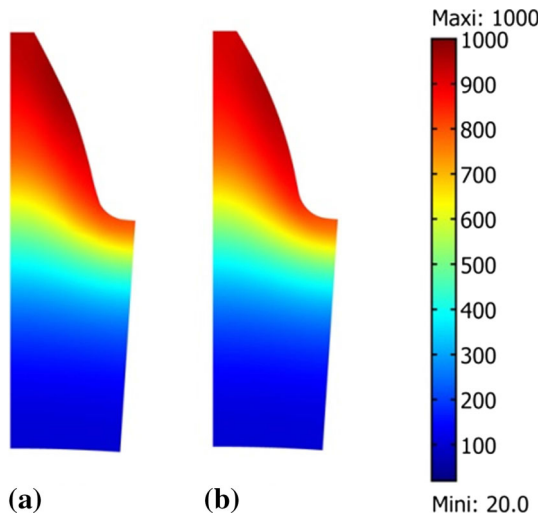


Fig. 9 Temperature distribution ( $^{\circ}\text{C}$ ) for  $\text{Gap}_z = 0$  mm: (a) Edge and (b) Middle plan—MF

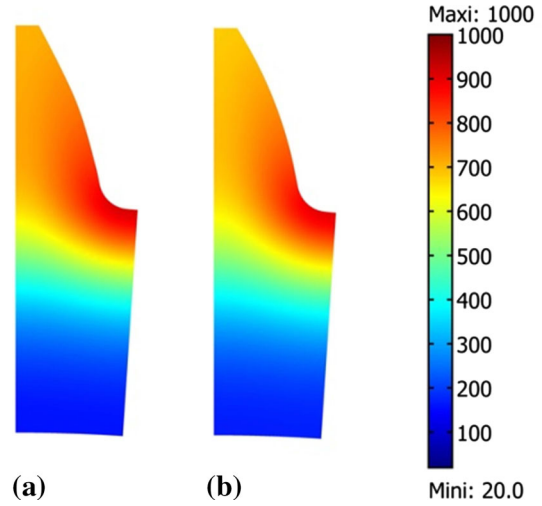


Fig. 10 Temperature distribution ( $^{\circ}\text{C}$ ) for  $\text{Gap}_z = 0$  mm: (a) Edge and (b) Middle plan—HF

temperature distribution and find the optimal value able to reduce the edge effect of the manufactured gear.  $J_0$  is adjusted at  $2.55 \times 10^{10}$  A/m<sup>2</sup> in MF case (10 kHz) and  $9.50 \times 10^{10}$  A/m<sup>2</sup> in HF case (200 kHz) in order to reach aso-called reference temperature fixed at 1000  $^{\circ}\text{C}$ . The heating time is fixed at 0.50 s.

Figures 9 and 10 present the simulation results where the flux concentrators are in permanent contact with the heated gear (there is no gap between the part and flux concentrators) for MF and HF respectively. The obtained results are very interesting and show at first sight that the edge effect is completely canceled. In this specific case, the temperature distributions are quite similar in MF and HF cases. These obtained results can justify the application of the proposed method applied early to cylindrical disk shape parts (Ref 8).

In a separate analysis, the gap between the gear and the flux concentrators was varied from 0 to 3 mm and the simulation was performed to analyze the temperature difference between the middle and edge plans in the tip and in the root of the gear tooth. Figure 11 and 12 present the temperature differences

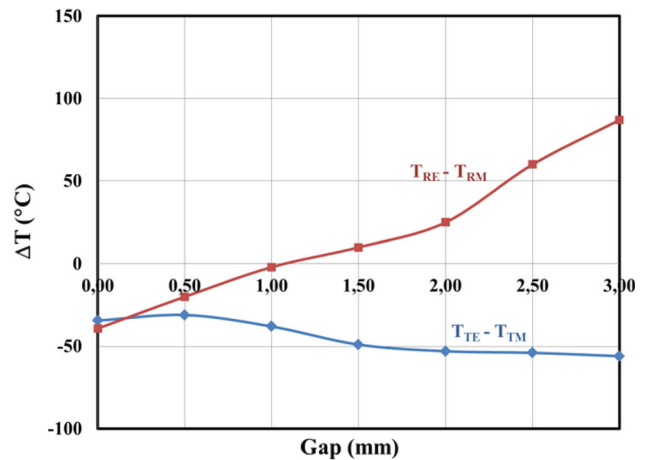


Fig. 11  $\Delta T$  vs. gap between gear and concentrators—MF

( $\Delta T_T = T_{TE} - T_{TM}$  and  $\Delta T_R = T_{RE} - T_{RM}$ ) versus  $Gap_z$  for both the MF and HF cases. It is important to note that, for both cases, the differences in temperature are minimal when the gap

is less than 0.5 mm. This value represents the optimal gap permitting to have the best uniform hardness profile using mono-frequency mode (MF and HF used separately).

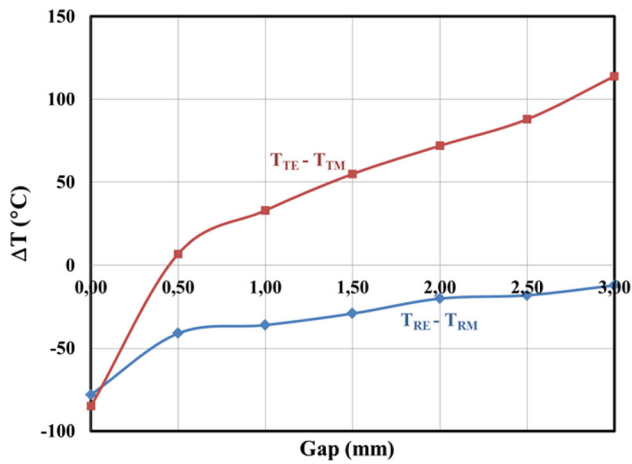


Fig. 12  $\Delta T$  vs. gap between gear and concentrators—HF

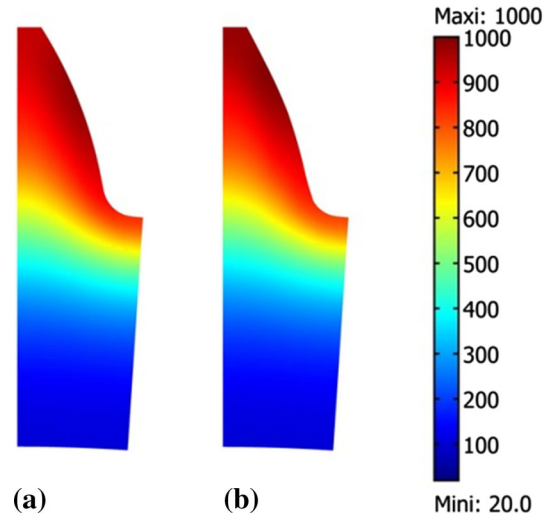


Fig. 15 Temperature distribution ( $^{\circ}\text{C}$ ): (a) Edge and (b) Middle—optimal heating

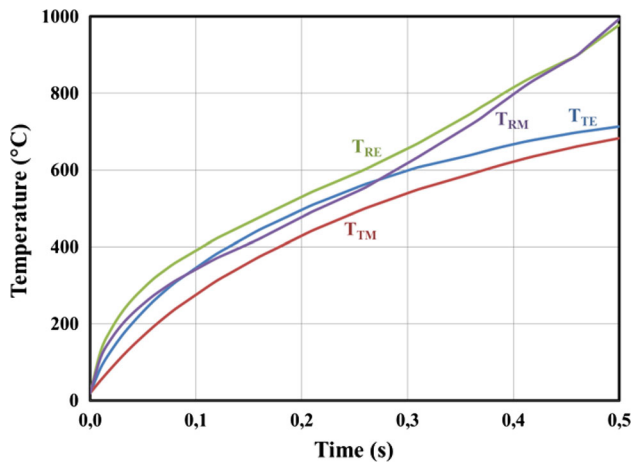


Fig. 13 Temperatures vs. time at MF—0.5 mm  $gap_z$

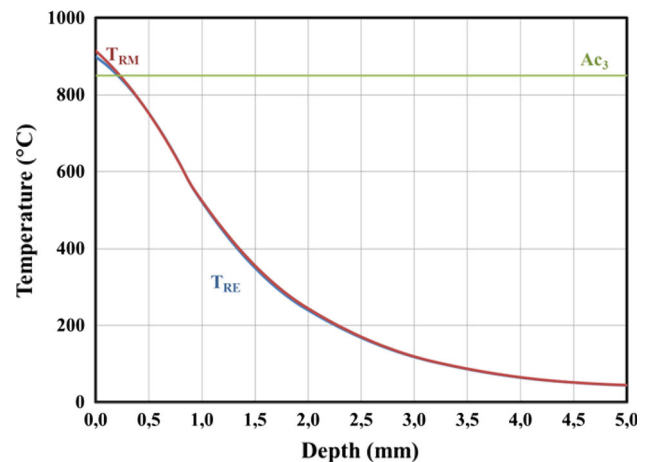


Fig. 16 Temperatures vs. depth—MF

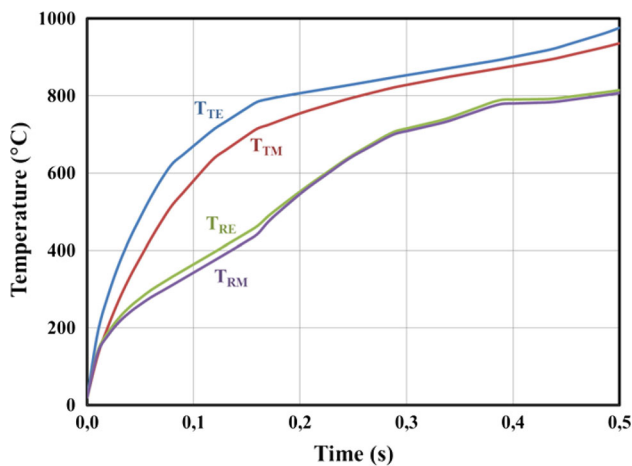


Fig. 14 Temperatures vs. time at HF—0.5 mm  $gap_z$

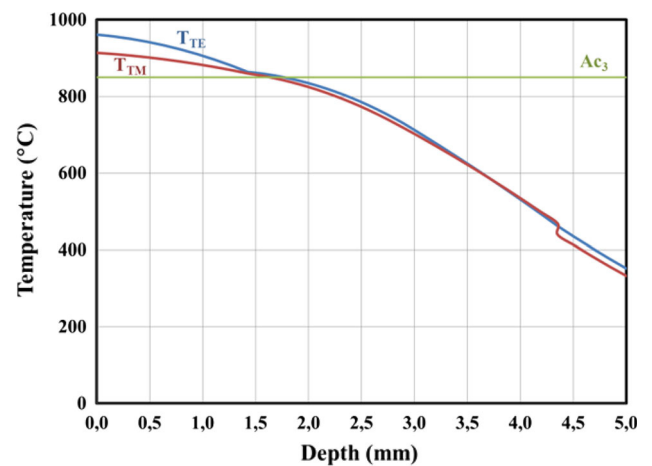
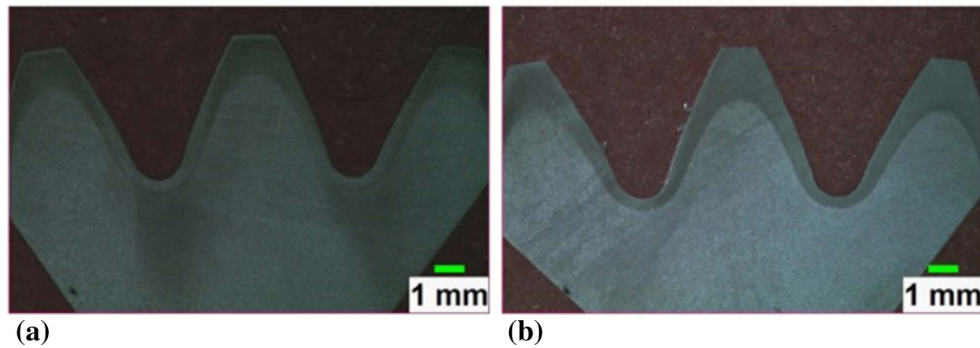


Fig. 17 Temperatures vs. depth—HF



**Fig. 18** Experimental hardness profile: (a) Edge and (b) Middle plane

The evolution of temperatures versus the depth was studied by carrying out simulation at the optimal case (gap 0.5 mm) for the both frequencies. Assuming that all regions were heated above  $A_{c3}$  (850 °C), it is possible to approximate the hardness curve in the tip and in the root of the gear. The temperature curves presented in Figs. 13 and 14 confirm that the temperature difference between the edge and the middle plan, for both root and tip positions, are closer to each other when the flux concentrators are used than in the original case (i.e., without flux concentrators).

#### 4. Optimized Temperature Profile

Since the gap is fixed to have better temperature profile without edge effect, it is interesting to combine the MF and HF to attempt reaching the best hardness profile. In this case, the MF mode is used to preheat the gear to 700 °C and the HF flash to allow for the transformation to take place. The idea is to reduce the heating time from 0.5 to 0.25 s for each frequency mode and keeping the same imposed current density as previously. Then, using a sequential heating with MF (initial current density of  $2.55 \times 10^{10}$  A/m<sup>2</sup> and 0.25 s) and HF ( $9.50 \times 10^{10}$  A/m<sup>2</sup> and 0.25 s), the temperature distributions at the middle plan and edge are almost the same. The obtained results are very interesting and show at first sight that is possible to eliminate completely the edge effect even if the tip receives more heat than the root (Fig. 15).

Finally, the evolutions of the four reference temperatures with the depth are presented in Fig. 16 and 17 at the end of the heating process. These curves give an approximation of the case depth. In fact, if the assumption stipulating that all regions heated above  $A_{c3}$  (850 °C) is considered, it is possible to approximate the case depths in the tip and the root of the gear. The case depths are 1.6 mm in the tip and 0.25 mm at the root. Moreover, the case depth at the tip appears to be more sensitive to changes in the imposed current density. The validation tests allow to confirm the concordance between simulation and validation concerning the utility to use flux concentrators (Fig. 18). In fact, the case depths in the edge are 0.3 mm at the root and 1.5 mm at the tip. The case depths are 1.6 mm at the tip and 0.3 mm at the root in the middle plan. It is also interesting to observe a ratio between case depth at the tip and that at the root and it is evaluated at about 5. The flux concentrators help to minimize greatly the edge effect, but it is important to find another method to make uniform the contour profile especially by increasing the frequency.

#### 5. Conclusion

This paper has presented an original and comprehensive approach permitting to reduce the edge effect on the hardness profile of spur gear and obtain the optimum hardness profile using finite element simulation. First, a 3D model was built using Comsol by coupling the electromagnetic and thermal fields. Second, the simulation model was also validated by a comparative analysis with experiments results. Finally, an optimization study was performed to eliminate the edge effect using additional gears acting as flux concentrators. The optimal gap between the part and flux concentrators permitting to eliminate the edge effect was then determined. By combining the MF and HF modes, it was shown that is possible to reach the optimum hardness profile. Overall, the obtained results show that simulation is useful also to understand the edge effect and how this phenomenon can be reduced. The application of such models will help induction-heating engineers to rapidly identify the optimum processing parameters for the induction machine and achieve the desired hardness profile. The developed method could be used also to optimize the surface treatment of spur gears. Other gears will be studied with the application of the flux concentrators in order to study the effect on the temperature distribution. This development exhibits a good potential to enhance the heating of complex geometries in industrial context. The use of flux concentrator presents a practical solution if validated for other geometries and if it is possible to reuse the same flux concentrator several times with the same performances.

#### References

1. L. Faure, *Aspect des dentures d'engrenages après fonctionnement*, 2nd ed., Publications CETIM, Paris, France, 1992, p 123
2. D.W. Dudley, *Handbook of Practical Gear Design*, CRC Press, Boca Raton, 1994, p 688
3. D. Tabor, *The Hardness of Metals*, Clarendon Press, Oxford, 1951, p 423
4. G.B. Olson and W.S. Owen, *Martensite*, ASM International, Materials Park, 1992, p 331
5. J. Grum and J. Mater, A review of the Influence of Grinding Conditions on Resulting Residual Stresses After Induction Surface Hardening and Grinding, *Processing Technol. Proc.*, 2001, **114**, p 212–226
6. N. Barka, A. Chebak, A. El Ouafi, P. Bocher, and J. Brousseau, Study of Induction Heating Process Applied to Internal Gear Using 3D Simulation, *Appl. Mech. Mater.*, 2012, **232**, p 730–735
7. N. Barka, P. Bocher, and J. Brousseau, Sensitivity Study of Hardness Profile of 4340 Specimen Heated by Induction Process Using Axi-

- symmetric Modeling, *Int. J. Adv. Manuf. Technol.*, 2013, **69**, p 2747–2756
8. N. Barka, A. Chebak, and J. Brousseau, Optimization of Hardness Profile of Bearing Seating Heated by Induction Process Using Axisymmetric Simulation, *Piers Online*, 2011, **7**, p 316–320
  9. V. Rudnev, D. Loveless, R. Cook, and M. Black, *Handbook of Induction Heating*, Marcell Dekker Inc., New York, 2003
  10. Y. Favennec, V. Labbe, and F. Bay, Induction Heating Processes Optimization a General Optimal Control Approach, *J. Comput. Phys.*, 2003, **187**, p 68–94
  11. J. Yuan, J. Kang, Y. Rong, and R.D. Sisson, Jr., FEM Modeling of Induction Hardening Processes in Steel, *J. Mater. Eng. Perform.*, 2003, **12**, p 589–596
  12. S. Zinn, *Elements of Induction Heating: Design, Control, and Applications*, ASM International, Metals Park, OH, 1988
  13. N. Barka, “Étude de sensibilité du profil de dureté des engrenages droits traités thermiquement par induction en fonction des paramètres machines,” École de technologie supérieure de Montréal, Ph.D. Thesis, p. 199, 2011
  14. W.D. Callister and D.G. Rethwisch, *Fundamentals of Materials Science and Engineering*, Wiley, New York, 2008, p 879